

Observation of Kondo resonance in YbAl_3

S.-J. Oh

Department of Physics, Seoul National University, Seoul 151, Korea

S. Suga, A. Kakizaki, M. Taniguchi, and T. Ishii

Synchrotron Radiation Laboratory, Institute for Solid State Physics, University of Tokyo, Tokyo 188, Japan

J.-S. Kang and J. W. Allen

Xerox Corporation, Palo Alto Research Center, 3333 Coyote Hill Road, Palo Alto, California 94304

O. Gunnarsson and N. E. Christensen

Max-Planck-Institut für Festkörperforschung, D-7000 Stuttgart 80, Federal Republic of Germany

A. Fujimori

National Institute for Research in Inorganic Materials, Sakura-mura, Niihari-gun, Ibaraki 305, Japan

T. Suzuki and T. Kasuya

Department of Physics, Tohoku University, Sendai 980, Japan

T. Miyahara and H. Kato

Photon Factory, National Laboratory for High Energy Physics, Ohomachi, Tsukuba-gun, Ibaraki 305, Japan

K. Schönhammer

Institut für Theoretische Physik, Universität Göttingen, D-3400 Göttingen, Federal Republic of Germany

M. S. Torikachvili and M. B. Maple

Institute for Pure and Applied Physical Sciences, University of California at San Diego, La Jolla, California 92093

(Received 5 June 1987; revised manuscript received 4 September 1987)

Anderson Hamiltonian parameters for mixed-valence YbAl_3 were determined from the magnetic susceptibility, photoelectron-spectroscopy, and bremsstrahlung-isochromat-spectroscopy data. The $4f^{13} \rightarrow 4f^{14}$ electron affinity energy is ~ 0.5 eV and the hybridization between Yb $4f$ and Al conduction electrons is ~ 0.05 eV, both of which are larger than conventional estimates. This hybridization and the resulting Kondo resonance are considered to play important roles for the anomalous properties of valence-fluctuating Yb compounds, as in the case of Ce compounds.

I. INTRODUCTION

Rare-earth and actinide compounds have been the subject of active research for the last few years. These compounds exhibit interesting phenomena such as mixed-valence and heavy-fermion properties,^{1,2} which are believed to originate from the highly correlated f electrons and their interaction with conduction-band electrons. Among these f -electron systems, Ce and its compounds are probably the most studied and best understood systems. Experiments such as photoelectron spectroscopy (PES) and bremsstrahlung-isochromat-spectroscopy (BIS) and theoretical efforts utilizing the large degeneracy N_f of the $4f$ level now firmly established³⁻⁵ that all known Ce metallic compounds are in the Kondo regime of the underlying Anderson Hamiltonian

$$H = \sum_{k,\sigma} \epsilon_k n_k + \sum_{m,\sigma} \epsilon_f n_{m\sigma} \sum'_{\substack{m,m' \\ \sigma,\sigma'}} U n_{m\sigma} n_{m'\sigma'} \\ + \sum_{k,m,\sigma} (V_{km} a_{m\sigma}^\dagger a_{k\sigma} + \text{H.c.}),$$

and the low-energy, low-temperature properties are controlled by spin fluctuations with an energy scale set by the Kondo temperature T_K . For example, the differences in physical properties between the α and γ phases of Ce metal and its compounds are now understood⁶ to reflect primarily the large change of T_K , rather than the gross change of $4f$ -electron occupation number n_f as had been believed for a long time.⁷ The variation of the $4f$ -conduction electron hybridization $\Delta = \pi \rho V^2$, where ρ is the conduction-band density of states, appears to be more important than the variation of the ionization energy ϵ_f or the f - f Coulomb energy U . PES and BIS measurements unambiguously show the existence of the narrow many-body Kondo resonance in the $4f$ spectral weight distribution,⁵ which is responsible for many anomalous physical properties. The scale of the Kondo resonance T_K is also the scale for the universal functions describing equilibrium, transport, and excitation properties of Ce impurities and compounds.⁸

It is natural to ask whether this success of the impurity Anderson Hamiltonian description can be extended to other anomalous rare-earth compounds as well. In par-

ticular, it is interesting to know how important the hybridization and the resulting Kondo resonance are for their anomalous physical properties. For heavier rare-earth mixed-valence compounds, Δ is traditionally expected to be small because of the lanthanide contraction of $4f$ wave functions, and the "promotional" model,⁷ where the change of ϵ_f and n_f is the controlling factor for their physical properties, is still commonly believed. To test the importance of the hybridization and the resulting Kondo resonance in these compounds, it is important to determine the parameter values of the Anderson Hamiltonian, particularly the $4f$ level energy ϵ_f and the hybridization strength Δ , since U is already known to be 6–7 eV. In this paper we report the results of the PES and BIS study on YbAl_3 , a typical mixed-valent Yb compound, to determine these parameter values ϵ_f and Δ . We chose to study YbAl_3 because (i) Yb ion, being the last element of rare-earth series, is expected to have smallest Δ , and (ii) Yb compounds can be treated conceptually in the same way as Ce compounds by simply interchanging the role of the $4f$ electron with that of the $4f$ hole.⁸ This is the first determination of these parameter values for mixed-valence rare-earth compounds other than Ce, and we found that contrary to common expectations the $4f$ level is substantially away from the Fermi level and that the hybridization still plays an important role for YbAl_3 just as in Ce cases.

II. EXPERIMENT

The sample was a polycrystalline ingot of YbAl_3 prepared by the induction-melting method. Polycrystalline LuAl_3 was also prepared by arc melting to get the reference spectra without $4f$ -electron contributions. Both crystals were annealed, and their crystal structures and stoichiometry were checked by the x-ray analysis. Fresh surfaces for PES and BIS measurements were obtained by fracturing the samples *in situ* with the base pressure better than 1×10^{-10} Torr. Oxygen and carbon contaminations were monitored during the measurements and found to be negligible. Valence-band photoemission spectra of YbAl_3 were measured using soft x-ray synchrotron radiation on the Beam Line 11-D of the Photon Factory in Japan, equipped with constant deviation monochromator⁹ and double-pass cylindrical mirror analyzer. Unoccupied densities of states (DOS) were measured at the Xerox Palo Alto Research Center, California, with the Vacuum Generators ESCALAB factory modified for BIS measurements. Valence-band PES spectra were taken at room temperatures, whereas BIS spectra were measured with samples cooled down by liquid nitrogen in order to reduce the contamination buildup during the measurement.

III. DATA AND INTERPRETATION

Figure 1(a) shows the valence-band photoemission spectrum of YbAl_3 at photon energy $h\nu = 100$ eV. The combined instrumental resolution (FWHM) due to the monochromator and the electron energy analyzer was 0.26 eV. The spectrum at this photon energy is dom-

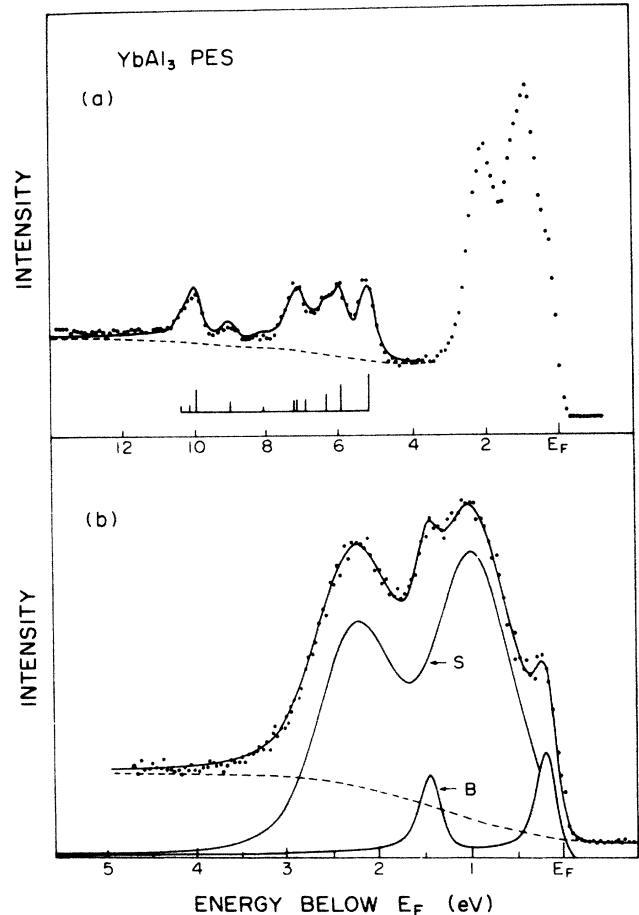


FIG. 1. Valence-band photoemission spectra of YbAl_3 and its theoretical fit. Dots are data points, the solid line is the theoretical fit, and the dashed line represents the inelastic background. (a) Wide scan at $h\nu = 100$ eV. The trivalent part is fitted with theoretical $4f^{13} \rightarrow 4f^{12}$ multiplet structures calculated in Ref. 10 (the energy scale is expanded by a factor of 1.1 to give the best fit) whose intensities are shown with bars. (b) High-resolution spectrum of the divalent part taken at $h\nu = 80$ eV. *B* and *S* represent the bulk and surface doublets, respectively. The singularity index α for the bulk peaks was set equal to 0.1, while that for the surface peak to zero.

inated by Yb $4f$ level emissions,¹⁰ so we can interpret this spectrum as the electron-removal part of the Yb $4f$ spectral weight in YbAl_3 . The structure between the Fermi level E_F and 4 eV below can be identified as the $4f^{14} \rightarrow 4f^{13}$ transition ("divalent" part), and that between 4 and 11 eV below E_F as the $4f^{13} \rightarrow 4f^{12}$ transition ("trivalent" part). This trivalent part is well fitted by the $4f^{12}$ final-state multiplet structures calculated by the coefficients of fractional parentage,¹¹ as shown in the figure by the solid line.

The divalent part consists of bulk and surface peaks, as can be seen clearly in the high-resolution data of Fig. 1(b). The instrumental resolution for this high-resolution spectrum¹² is 0.15 eV, and here the least-square fit shows two sets of $4f^{13}$ spin-orbit doublets (spin-orbit splitting $\Delta_{SO} = 1.27$ eV, intensity ratio = $\frac{3}{4}$) separated from each other by 0.79 eV. The narrow dou-

blet at lower binding energy is from the bulk $4f^{14} \rightarrow 4f^{13}_{7/2}, 4f^{13}_{5/2}$ transitions, and the broad one at higher binding energy is from the totally divalent surface layers, as in the case of YbAl_2 .¹³ The fact that this second doublet is the surface feature was also confirmed by the oxygen test. These surface shifted peaks were not resolved in earlier XPS data¹⁴ on YbAl_3 due to inadequate resolution and some oxygen contaminations. The intrinsic width (FWHM) of the bulk $4f^{13}$ peak obtained from the fit is less than 0.2 eV, whereas the surface peaks are more than 0.8 eV wide, probably due to the fact that many different crystal orientations exist at the surface and more than one surface layer contributes to this peak.¹³ The valence of the bulk YbAl_3 at room temperature deduced from the intensity ratio of the trivalent part and the *bulk* divalent part is 2.78 ± 0.03 . This value is a little smaller than the value $\nu = 2.95$ estimated from the lattice constant measurement,¹⁵ but consistent with the estimate of 2.75 from the L_{III} absorption-edge spectra.¹⁶ We believe that this discrepancy is due to the inadequacy of the linear Vegard's law used to determine the valence from the lattice constant,¹⁶ and that our estimate based on the photoemission intensity is more reliable. We note, however, that this estimate neglects the dynamical effect of the hybridization,⁴ which is expected to be small for the parameter range of YbAl_3 determined below.

Figure 2 shows the BIS spectrum of YbAl_3 taken with $h\nu = 1486.6$ eV (dots). To extract Yb $4f$ spectral weight, we also measured the LuAl_3 BIS spectrum shown in the figure with the solid line. The instrumental resolutions for these spectra are ~ 0.4 eV, and the two spectra are scaled so that the intensities at ~ 5 eV above E_F are

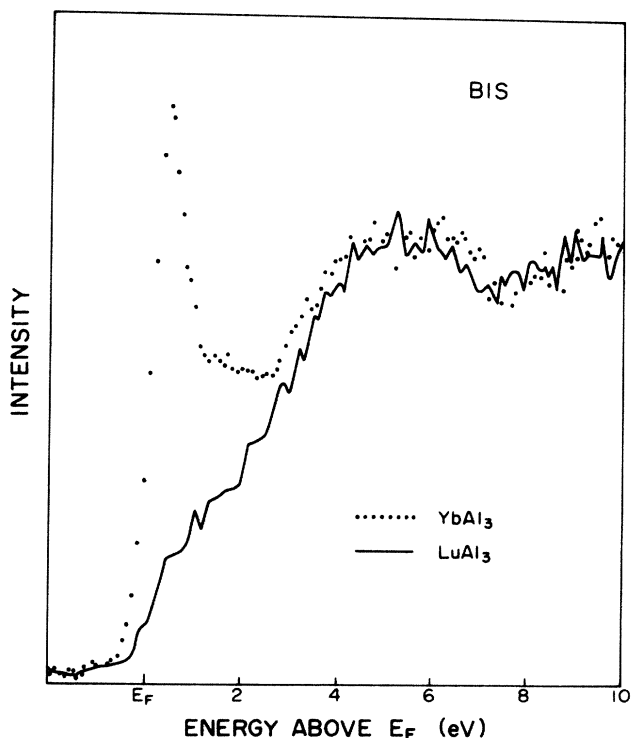


FIG. 2. BIS spectra of YbAl_3 (dots) and LuAl_3 (solid line).

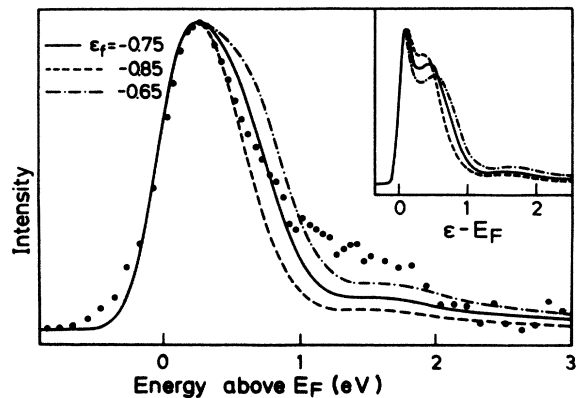


FIG. 3. Experimental Yb $4f$ spectral weight (dots) compared with the Gunnarsson-Schönhammer model theoretical fit (solid line) in the energy range 0–3 eV above E_F . A Gaussian broadening of 0.4 eV (FWHM) was used to simulate the experimental resolution. The inset shows the theoretical curve with a reduced Gaussian broadening (FWHM=0.15 eV). Dashed and dot-dashed lines are theoretical curves when the ϵ_f value is changed by ± 0.1 eV (see text).

equal. The Yb $4f$ spectral weight was then obtained by subtracting LuAl_3 data from the YbAl_3 spectrum, the result of which is shown in Fig. 3 with dots. We note the following features in this difference spectrum (1) there are two structures in the Yb $4f$ spectral weight—a peak near the Fermi level (between 0 and 1 eV above E_F) and a shoulder between 1 and 2 eV. These two structures are clearly distinguished by the slope change at about 1 eV above E_F . The shoulder between 1 and 2 eV above E_F is not an artifact of our subtraction procedure, as other reasonable procedures we tried always gave a substantial $4f$ weight in this energy range. (2) The peak near the Fermi level (between 0 and 1 eV above E_F) is asymmetric in shape in that the slope of the leading edge is entirely determined by the instrumental resolution whereas the descent above the peak is slower, giving an indication of the intrinsic width on the higher-energy side.

These two experimental features cannot be explained by the simple promotional model, where the $4f$ level is “pinned” at the Fermi level to give mixed valency and the anomalous physical properties for YbAl_3 . In this promotional model, $4f$ spectral weight of YbAl_3 in the BIS spectrum would be a single peak at E_F , which is essentially symmetric within the experimental resolution.¹⁷ On the contrary, we will show below that the recently proposed theory for calculating $4f$ spectral weights of the Anderson Hamiltonian^{4,18} can account for these two essential features of YbAl_3 BIS spectrum, and that the parameter values so determined are in the range where the hybridization and Kondo resonance are important for understanding its anomalous physical properties.

IV. THEORETICAL FIT

In the spin fluctuation limit of the Anderson Hamiltonian with $U \rightarrow \infty$ and $N_f \rightarrow \infty$, there exist the follow-

ing exact analytic relations:^{4,19}

$$\chi(0) = \frac{1}{3} \frac{\mu_{\text{eff}}^2 n_f}{\delta}, \quad \delta = B \exp \left[-\frac{\pi |\varepsilon_f|}{N_f \Delta} \right],$$

$$\frac{n_f}{1-n_f} = \frac{N_f \Delta}{\pi \delta}$$

that enables us to determine ε_f and Δ if one knows the valence v and the zero-temperature magnetic susceptibility $\chi(0)$. Here $\mu_{\text{eff}} = \sqrt{j(j+1)} g_j \mu_B = 4.54 \mu_B$ for the $4f^{13}$ configuration, n_f is the number of the $4f$ hole, B is the bandwidth, and δ is the Kondo temperature. Since the experimental value of $\chi(0)$ for YbAl_3 has been reported previously,¹⁵ we can try to estimate ε_f and Δ using the value of valence determined above. However, inclusion of spin-orbit splitting, finite U , and charge fluctuation effects modifies these estimates, and a theory was developed earlier by two of us^{18,4} using the method of $1/N_f$ expansion. We therefore used this theory to determine parameter values of ε_f and Δ that give theoretical v and $\chi(0)$ which are consistent with the experimental results. This theory also predicts the $4f$ spectral weight distribution, and we show in Fig. 3 with the solid line the theoretical curve with parameter values thus determined. We see that this theoretical fit reproduces the above-mentioned two essential features of the experimental spectrum reasonably well—an asymmetric peak near the Fermi level and an extra structure at 1–2 eV above E_F , with a slope change around 1.2 eV.

The parameters of the fit are $U = 7$ eV, $\varepsilon_{f5/2} = -0.75$ eV, $\Delta_{\text{SO}} = \varepsilon_{f7/2} - \varepsilon_{f5/2} = 1.27$ eV, and $\Delta_{\text{av}} = 0.05$ eV where Δ_{av} denotes the average of the hybridization strength $\pi \rho |V(\varepsilon)|^2$ over the conduction band. These parameters give the valence²⁰ $v = 2.79$ consistent with the value determined by our PES spectrum, and the zero-temperature magnetic susceptibility $\chi(0) = 4.60 \times 10^{-13}$ cm³/mole of the Yb atom, in good agreement with the experimental value of 4.62×10^{-13} cm³/mole. To show the sensitivity of the fit to the change of parameter values, we also show in Fig. 3 the theoretical curves for $\varepsilon_f = -0.65$ eV (dot-dashed) and $\varepsilon_f = -0.85$ eV (dashed), maintaining the same valence $v \cong 2.78$ by adjusting Δ_{av} accordingly ($\Delta_{\text{av}} = 0.056$ eV for the dot-dashed line and $\Delta_{\text{av}} = 0.034$ eV for the dashed line). We see that these small changes of ε_f by ± 0.1 eV make the overall agreements worse, and furthermore $\chi(0)$ for these cases are 3.5×10^{-13} and 6.0×10^{-13} cm³/mole, respectively, in substantial disagreement with the experimental value. That is, the theoretical $4f$ spectral weight curve with parameters ε_f and Δ which are consistent with experimental v and $\chi(0)$ also gives the most reasonable fit of the BIS spectrum in YbAl_3 .

The asymmetry of the peak near E_F is due to its intrinsic structure, as confirmed by the theory curve with the same parameters but with a reduced Gaussian broadening (0.15 eV) shown in the inset of Fig. 3. This curve shows a “Kondo peak” at the Fermi energy and a second shoulder at ~ 0.5 eV corresponding to the $4f^{13}(^2F_{7/2}) \rightarrow 4f^{14}(^1S_0)$ transition. In the analogy between the Yb BIS and the Ce PES spectrum,⁸ this peak

corresponds to the Ce f^0 peak (at about -2 eV) in the PES spectrum.

The structure at 1–2 eV above E_F is related to the spin-orbit splitting of the Yb $4f^{13}$ configuration. As Bickers *et al.*⁸ first pointed out, the upper spin-orbit feature in the Yb BIS spectrum can give rise to an antiresonance because of the interference with the “ionization” peak at $\varepsilon_{f7/2}$. The minima at $\Delta_{\text{SO}} \cong 1.2$ eV due to this antiresonance are all seen in theory curves of Fig. 3. The fact that this structure is due to the spin-orbit energy is confirmed by Fig. 4, where we show two theory curves with the same $\varepsilon_{f7/2}$ values (~ 0.55 eV) but with different spin-orbit energies ($\Delta_{\text{SO}} = 1.2$ eV for the solid line, and $\Delta_{\text{SO}} = 1.5$ eV for the dotted line). We can see that the minimum and the peak above it moved by about 0.3 eV, the difference between two spin-orbit energies used. The fact that the experimental $4f$ spectrum shows this feature at 1–2 eV above E_F supports our interpretation that the peak at E_F is not just the $4f^{14}$ final state but must involve the $4f^{13}$ final state as well.

The theoretical curve for the Yb $4f$ BIS spectrum in Fig. 3 was generated by the theory developed earlier for Ce compounds PES (Ref. 4) by interchanging the hole and electron parts of the spectrum. This calculation of the $4f$ BIS spectrum and the susceptibility $\chi(0)$ was performed to the lowest order in $1/N_f$, and the effect of finite U was also included.^{18,4} Since Yb $4f$ electrons are expected to hybridize mainly with the nearest-neighbor Al states, we calculated the partial density of Al spd states in LuAl_3 by the linearized muffin-tin orbital (LMTO) method and took the result as the conduction band density of states. This partial density of Al spd states is shown in Fig. 5, and it is found to be substantially different from the experimental LuAl_3 BIS spectrum of Fig. 2. This is due to the contribution from Lu

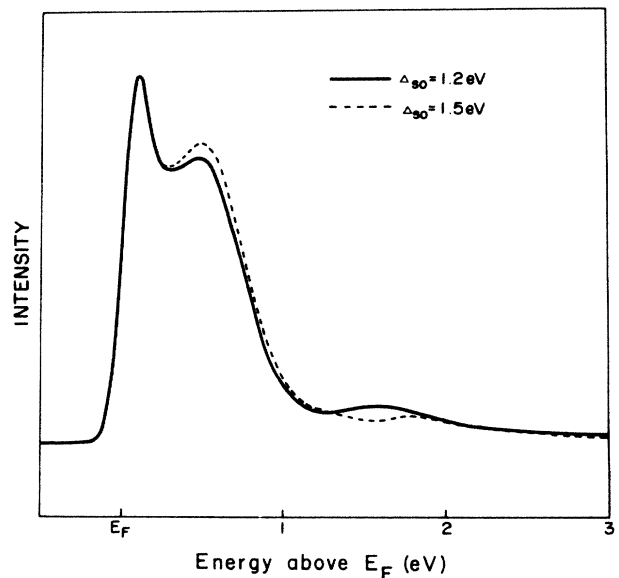


FIG. 4. Comparison of two theoretical curves with the same $\varepsilon_{f7/2} = 0.55$ eV and $\Delta_{\text{av}} = 0.05$ eV but with different spin-orbit energies. ($\Delta_{\text{SO}} = 1.2$ eV for the solid line and $\Delta_{\text{SO}} = 1.5$ eV for the dotted line). Gaussian broadening of 0.15 eV was used.

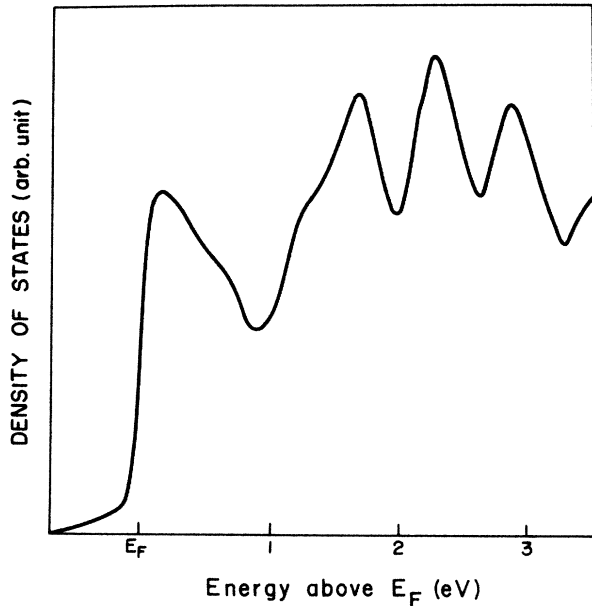


FIG. 5. Partial density of Al spd states in LuAl_3 used for the calculations of the $4f$ BIS spectrum and the susceptibility. This density of states was calculated by the linearized muffin-tin orbital (LMTO) method.

$5d$ states, which has a large cross section at this photon energy.¹⁰ The conduction band was cut off at 3 eV above E_F in the calculations for numerical reasons, which introduces slight renormalizations of the ϵ_f and Δ_{av} values quoted above. The hybridization parameter V_{km} was assumed to be the same throughout the band.

The ϵ_f and Δ_{av} values determined above may seem surprisingly large. To understand this better, we performed the band-structure calculations of both LuAl_3 and LaAl_3 and compared their bonding parameters. We found that although p - f bonding parameters of LuAl_3 are indeed smaller than those of LaAl_3 by about a factor of 4, the mixing of the Lu $4f$ state with the free-electron-like part is not so much different.²¹ This suggests that ϵ_f and Δ_{av} values determined above are not unreasonable.

One discrepancy between the experimental $4f$ spectral weight and the theoretical fit in Fig. 3 is the amount of

the weight in the energy range 1–2 eV above E_F . This discrepancy may be due to several simplifications made in the theory. One is, of course, the use of the simple Anderson model Hamiltonian to describe the complicated real physical system, and others may be the effects of higher-order terms in $1/N_f$. But what is likely to be more important is the fact that we neglected the Yb $5d$ - $4f$ hybridization between next-nearest neighbors and also the detailed variations of $|V(\epsilon)|^2$ in the conduction band.²¹ In fact, this is the region where the shape of $|V(\epsilon)|^2$ is found to give significant changes in the position and weight of $4f$ spectral weights in the Ce compound PES spectrum.³ However, this discrepancy at 1–2 eV is only quantitative, which hopefully can be improved by a more detailed theory. What is important here is the fact that we were able to describe essential features of spectroscopic data (PES, BIS) and relate to the thermodynamic property $[\chi(0)]$ with *one model* with *the same* parameters.

V. CONCLUSIONS

We have determined parameter values of the Anderson Hamiltonian for YbAl_3 that give a consistent description of the magnetic susceptibility, photoemission, and BIS spectra. The $4f$ electron affinity energy ϵ_f and the hybridization Δ_{av} are considerably larger than traditional estimates, although they are indeed smaller than most anomalous Ce compounds as expected from the lanthanide contraction. The large hybridization and resulting Kondo resonance are considered important for anomalous physical properties of valence-fluctuating Yb compounds, and features of Kondo resonance and its sidebands are seen in the $4f$ spectral weight distribution measured by PES and BIS.

ACKNOWLEDGMENTS

One of us (S.J.O.) gratefully acknowledges the travel grant provided by the Yamada Foundation, Korea Science and Engineering Foundation (KOSEF), and Japan Society for the Promotion of Science (JSPS). Research in the U.S.A. (J.S.K., J.W.A., M.S.T., and M.B.M.) was supported by the U.S. National Science Foundation under Grant No. DMR-84-11839.

¹For recent reviews, see, for example, J. M. Lawrence *et al.*, Rep. Prog. Phys. **44**, 1 (1981); P. A. Lee *et al.*, Comments Cond. Mat. Phys. **12**, 99 (1986).

²*Theory of Heavy Fermions and Valence Fluctuations*, edited by T. Kasuya and T. Saso (Springer-Verlag, New York, 1985).

³J. W. Allen, S.-J. Oh, O. Gunnarsson, K. Schönhammer, M. B. Maple, M. S. Torikachvili, and I. Lindau, Adv. Phys. **35**, 275 (1986).

⁴O. Gunnarsson and K. Schönhammer, Phys. Rev. B **28**, 4315 (1983); *ibid.* **31**, 4815 (1985).

⁵J. W. Allen, S.-J. Oh, M. B. Maple, and M. S. Torikachvili, Phys. Rev. B **28**, 5347 (1983).

⁶J. W. Allen and Richard M. Martin, Phys. Rev. Lett. **49**, 1106 (1982).

⁷W. H. Zachariasen, Phys. Rev. **76**, 301 (1949); L. Pauling, J.

Chem. Phys. **18**, 145 (1950).

⁸N. E. Bickers, D. L. Cox, and J. W. Wilkins, Phys. Rev. Lett. **54**, 230 (1985).

⁹T. Miyahara *et al.*, Jpn. J. Appl. Phys. **24**, 293 (1985).

¹⁰S. M. Goldberg, C. S. Fadley, and S. Kono, J. Electron Spectrosc. Relat. Phenom. **21**, 285 (1981).

¹¹F. Gerken, J. Phys. F **13**, 703 (1983).

¹²This spectrum was taken at $h\nu=80$ eV, but the spectrum at $h\nu=100$ eV is similar, except that the intensity ratio between surface and bulk peaks is somewhat different, presumably due to the different electron escape depth.

¹³G. Kaindl *et al.*, Solid State Commun. **41**, 157 (1982).

¹⁴K. H. J. Buschow, M. Campagna, and G. K. Wertheim, Solid State Commun. **24**, 253 (1977).

¹⁵J. C. P. Klaasse, F. R. DeBoer, and P. F. De Châtel, Physica

- B + C **106B**, 178 (1981).
- ¹⁶D. Wohlleben, in *Moment Formation in Solids*, edited by W. J. L. Buyers (Plenum, New York, 1984), p. 171.
- ¹⁷S.-J. Oh and J. W. Allen, *Phys. Rev. B* **29**, 589 (1984).
- ¹⁸O. Gunnarsson and K. Schönhammer, in *Theory of Heavy Fermions and Valence Fluctuations*, Ref. 2, p. 110.
- ¹⁹D. N. Newns, A. C. Hewson, J. W. Rasul, and N. Read, *J. Appl. Phys.* **53**, 7877 (1982).
- ²⁰The experimental valence was obtained at room temperature, whereas this theoretical valence is at $T=0$. However, the difference is expected to be small judging from the lattice parameter as a function of temperature [see A. Iandelli and A. Palenzona, *J. Less-Common Met.* **29**, 293 (1982)].
- ²¹K. Takegahara, M. Takeshige, and T. Kasuya (unpublished).